Preparation and characterization of VO_x/TiO_2 catalytic coatings on stainless steel plates for structured catalytic reactors.

Thierry Giornelli, Axel Löfberg* and Elisabeth Bordes-Richard

Unité de Catalyse et de Chimie du Solide, UMR-CNRS 8181, USTL-ENSCL, Bât. C3, Cité Scientifique, 59655 Villeneuve d'Ascq, France.

*Corresponding author. Tel: +33-320434527

Fax: +33-320436561

E-mail address: Axel.Lofberg@univ-lille1.fr

Abstract

The parameters to be controlled to coat metallic walls by VO_x/TiO_2 catalysts which are used in the mild oxidation of hydrocarbons and NO_x abatement are studied. Stainless steel (316 L) was chosen because of its large application in industrial catalytic reactors. TiO_2 films on stainless steel were obtained by dip-coating in two steps. Superficially oxidized plates were first dipped in Ti-alkoxide sol-gel to be coated by a very thin layer of TiO_2. On this anchoring layer was then deposited a porous film of titania by dipping plates in an aqueous suspension of TiO_2 particles. After calcination, VO_x species were grafted to TiO_2/SS plates and their loading was determined by means of X-ray Photoelectron Spectroscopy. The chemical and mechanical resistances of films were controlled by several tests. Laser Raman Spectroscopy, X-Ray Diffraction and Scanning Electron Microscopy were used to characterize the samples after each step of preparation. The porous texture was determined using a thermobalance. The dispersion and the nature of VO_x species and the value of theoretical monolayer of VO_x on

TiO_2/stainless steel are shown to depend on the surface V/Ti ratio, in the same manner as for VO_x/TiO_2 coating anodised aluminum plates and as for VO_x/TiO_2 powders, . Therefore, we have demonstrated that the shaping of TiO_2 has no influence on the characteristics of the active phase, which is of prime importance for catalytic applications in structured reactors.

Keywords: structured reactors, catalytic wall reactors, stainless steel, dip-coating, V_2O_5/TiO_2 catalyst, XPS.

1. Introduction

Heat exchanger type reactors are studied till recently because of their potential applications in highly exothermic reactions [1, 2] like, for example, the oxidative dehydrogenation of C_2-C_4 alkanes [3-6]. Compared to fixed bed reactors in which heterogeneous catalytic reactions are most often carried out, structured reactors could be profitably used because the heat transfer between the poorly conducting oxidic material and the metallic wall would be better controlled [7]. In such cases, the catalytic active phase must be deposited onto the metallic plates that constitute the reactor walls, or directly onto the walls, according to the reactor design. Obviously, this assembly must be mechanically and thermally stable, chemically resistant to the reactants, while the coating must retain its specific textural and catalytic properties. Once the active oxidic material is chosen, the coating procedure must be adapted case by case according to the nature of the metallic substrate (e.g., aluminum or stainless steel) and, eventually, its shape.

We have recently studied the coating of aluminum plates with VO_x/TiO_2 catalyst [8]. This catalyst is well-known to be active and selective in several types of reactions like the mild oxidation of hydrocarbons (o-xylene oxidation to phthalic anhydride, oxidative dehydrogenation of propane, etc.) as well as in pollution abatement (selective catalytic reduction of NO_x by ammonia). Aluminum is a good thermal conductor (237 $W.m^{-1}.K^{-1}$). Its surface is naturally covered by a layer of alumina which may serve as an anchoring layer for other oxides [9]. As its porosity can be increased by anodization, high surface area coatings are expected. Among other V/Ti compositions we studied, a monolayer of VO_x onto anatase, itself coating anodized Al, was deposited by dip-coating of the plates in a sol-gel of Ti-alkoxide precursor. Dipping in sol-gel medium is

one of the most appropriate ways to prepare thin oxide coatings because of several advantages, among which a high homogeneity, an easy control of composition and a low processing temperature. After grafting TiO_2 onto alumina, we thought that a high amount of porous titania layers could be deposited on plates, in particular by using a porogenic agent. However, we have demonstrated by varying several parameters [8], that it is not possible to obtain films with well defined porous structures because of a demixtion phenomenon occuring at the solution-plate interface. This work illustrated the difficulties encountered when transposing technologies initially developed for powders to plate-supported catalysts.

The coating of stainless steel plates with VO_x supported on titanium dioxide (anatase) is presented here. Even if its thermal conductivity (46 $W.m^{-1}.K^{-1}$) is lower than that of aluminum, stainless steel stands high temperatures and is the preferred material of most industrial reactors. Obviously this metal cannot be anodised, and consequently it is not easy to get a porous oxide layer onto which TiO_2 films could be anchored. Therefore, we have adapted the method elaborated to make $TiO_2/Al_2O_3/Al$ by using a suspension of TiO_2 powder to coat stainless steel once a thin layer of titanium dioxide has been grafted. The hypothesis is that, after deposition, the titanium dioxide film will present the same properties than the initial corresponding powder. Such suspensions of TiO_2 (generally TiO_2-P25 from DEGUSSA) have already been proposed for the coating of glass plates [10-13]. Two main applications are photocatalysis for the decomposition of organic compounds in waste water [14, 15], and optical thin films because of the high refractive index and the chemical stability of TiO_2 [16, 17]. Fernandez et al. [18] and Byrne et al. [19] have used the electrophoretic method for such coating on stainless steel but, up to our knowledge, there is no paper concerning the deposition of anatase on stainless steel by dip-coating in suspensions of TiO_2. The anatase form is preferred for

catalytic applications because its strong interaction with vanadium oxide allows to generate a molecular dispersion of VO_x oxide layer, which exhibits the best activity and selectivity in most reactions [20].

In this paper we report on the grafting of VO_x monolayer on TiO_2-anatase coated stainless steel plates. The characterization of the deposits at the various stages of the preparation suffers from several difficulties because of the large contribution of the metallic plate, whereas most of the experimental equipments used in the field of catalysis are designed for powders. As developed in a previous paper [8], we have used X-ray Photoelectron Spectroscopy (XPS) which allows to control and to quantify the amount of active phase VO_x as well as of TiO_2 deposited on metallic plates. The structural properties of coated plates have been studied by Scanning Electron Microscopy (SEM), Laser Raman Spectroscopy (LRS), and their texture has been analysed using the Brunauer-Emmet-Teller (BET) method. Results will be compared to those obtained in [8] for $VO_x/TiO_2/Al_2O_3/Al$ as well as with powders of VO_x/TiO_2 which have also been prepared.

2. Experimental procedure

2.1. Physicochemical analyses

The specific surface area and the porosity of the film on plates at various stages of coating were determined from the nitrogen adsorption and desorption isotherms, to which the BET method was applied. The partial pressure of nitrogen varied from 10^4 to 10^5 Pa at 77 K. All samples were first degassed at 150°C for 4 h in vacuum. Because of the large weight and size of the metal plate as compared to that of the coating, these

isotherms were obtained using a thermobalance (Sartorius GmBH, model S3D-V), the reference being a bare stainless steel plate of the same size. For the same reason, it is more appropriate to consider the developed surface area – as compared to the geometric surface area of the plate – instead of the specific surface area.

Laser Raman spectra were recorded on a LabRAM Infinity spectrometer (Jobin Yvon) equipped with a liquid nitrogen detector and a frequency-doubled Nd:YAG laser supplying the excitation line at 532 nm. The power on the sample was less than 5 mW. The spectrometer was calibrated daily using the silicon line at 521 cm^{-1}.

After grafting or coating, VO_x and TiO_2 deposits were analyzed by XPS using Leybold VG Escalab spectrometer. The residual pressure in the ultra-high vacuum chamber was about 10^{-9} Pa. Al Kα X-ray source was used to study VO_x/TiO_2/stainless steel plates. The spectra were referenced to O1s photopeak (from TiO_2) with binding energy BE = 530 eV.

Surface images were obtained by means of Hitachi 4100 S scanning electron microscope equipped with a Field Emission Gun, with numerical image acquisition.

X-Ray Diffractograms (XRD) were obtained by reflection with a Siemens D5000 diffractometer (Cu $K\alpha_1$ line, λ = 154.2 ppm). The $K\alpha_2$ line contribution was eliminated by mathematic treatment with the software Eva ver. 9.0 (Brucker Advanced X-Ray Solutions).

The mechanical and chemical resistances of the films were studied according to two qualitative tests:

- Test 1: The adhesion of coatings was investigated by means of a piece of adhesive tape (Scotch 3M) sticked onto the surface. The tape was firmly rubbed with

finger tip and removed. Only oxide coatings with no particles left on the adhesive tape were further processed [21].

- **Test 2:** Plates were introduced in the thermobalance after a precise weighing. Temperature cycles (10°C/min) were successively performed under different atmospheres (air, nitrogen, hydrogen). The temperature was held at 200°C during 12 h, then decreased to room temperature and again increased up to 500°C (12 h). .

2.2. Preparation of plates before the film deposition

Stainless steel 316L is an austenitic alloy containing 18% of chromium, 13% of nickel and 2.5% of molybdenum (Table 1), the later being used to decrease the sensitivity to corrosion. Passivation oxides like $(Fe,Cr)_2O_3$ are present on the surface (Figure 1), but their developed surface area (m^2 per geometrical m^2 of plate) is practically the same than the geometric surface area of stainless steel.

Plates (5 cm × 2 cm × 0.5 mm) of 316L were chemically treated by a sulphuric acid solution (30 wt%) during 2 h in order to increase the roughness of the surface oxides [22-24]. In order to eliminate acidic traces before the anatase film deposition, plates were sonicated two times in water during 30 minutes and left standing at room temperature during 3h. On the resulting plate (noted **SSH)** examined by SEM (Figure 2), the rugosity was seen to increase after treatment, the passivation film being mainly developed on the grains and not on grain boundaries. XPS experiments confirmed the increased thickness of the passivation film. From the metallic ratio ($X_i = \left(\frac{\%\, M_i}{\sum \%\, M_i} \right)$, where M_i is the atomic percentage of the metal "i" = Fe, Cr, Mo), it is clearly seen on Table 2 that X_{Fe} decreases from 0.8 to 0.5 after the acidic treatment, while X_{Cr} increases from 0.15 to 0.5. The binding energy (BE) at 711.0 eV for Fe 2p , 577.1 eV for Cr 2p

and 233.0 eV for Mo 3d correspond to Fe^{3+}, Cr^{3+} and Mo^{6+} in their respective oxides [25, 26].

Before and after the acidic treatment, the XRD patterns of SSH remained unchanged, confirming the fact that the corrosion affected only the surface of the samples.

2.3. Coating of plates

1rst step: Deposition by sol-gel

The precursor solutions were prepared according to Giornelli et al. [8]: 17.2 ml of tetrabuthylorthotitanate $Ti(OBu)_4$ 97% and 4.8 ml of diethanolamine 99% (both SIGMA-ALDRICH) were dissolved in dry ethanol (67.28 ml) (FLUKA). The solution was stirred vigorously at room temperature for 2 h. 2.7 ml of water and 10 ml of ethanol ($Ti(OBu)_4$:C_2H_5OH:H_2O:$NH(C_2H_4OH)_2$ = 1:25.5:3:1, molar ratio) were added dropwise to the solution under stirring. The resultant alkoxide sols were left standing at room temperature for two hours for the hydrolysis reaction to proceed. TiO_2 films were prepared by dipping (20 s) and withdrawing the **SSH** plates at 6 $mm.s^{-1}$. The resulting plates, noted **SSHT,** were calcined in a furnace in air flow at 80°C.h^{-1}, up to 100°C during 1 h and then at 900°C for 2 h.

2nd step: Deposition of a porous film of TiO_2 by suspension on **SSHT**

In order for a film of TiO_2 to be homogeneous, the size distribution of oxide particles in suspension must be as narrow as possible. Several commercial samples of TiO_2-anatase powders were analysed by a granulometer (LS Coulter). Hombikat-T particles of TiO_2 (50 m^2/g, size 50 µm) flocculated in the beaker and the sample was discarded. The particle size distribution of TiO_2-Aldrich (10 m^2/g) being more narrow

(size range 0-250 µm) than that of TiO_2-Alfa-Aesar (52 m^2/g, 0-1500 µm),TiO_2-Aldrich powder was chosen for the suspension.

Several tries were realized on the basis of those described in the literature [27-29], by varying numerous parameters like the medium (water, diluted nitric acid, surfactant addition), the amount of TiO_2 in suspension, the time of immersion [30]. In most cases, the films were less than 1 µm thick and/or did not stand the stability tests. Finally, the following procedure led to stable and thick enough deposits: **SSHT** samples were dipped under stirring 5 min in 60 wt% of TiO_2 particles suspended in water, and withdrawn at 6 $mm.s^{-1}$. Plates were calcined 1 h up to 110°C, and then 2 h at 900°C (80°C/min) in air flow. The latter temperature was chosen after dilatometric experiments (see below). The resulting samples are noted **T/SSHT.**

3rd step: Grafting of VO_x specie on T/SSHT

Vanadium(V)-oxytripropoxide $VO(OPr)_3$ 98% (SIGMA-ALDRICH) was used as precursor. Solutions containing different amounts (C = wt% of $VO(OPr)_3$ in dry ethanol) of precursor were prepared. T/SSHT plates were dipped under stirring during 1 h, and then withdrawn (6 $mm.s^{-1}$) from the solution. The plates were then heated in a furnace (30°$C.h^{-1}$) at 450°C for 4 h in air flow. Resulting samples were noted **VT/SSHT.**

3. Results and discussion

3.1. Stainless steel plates (SSHT)

SEM micrographs of SSHT plates show clearly that the surface of SSH is

modified after the grafting of Ti alkoxide and calcination, which is in favour of the presence of an anchoring titania layer on the surface of SSH (Figure 3).

The BE of Fe 2p, Ti 2p, Mo 3d, Cr 2p, Mn 2p photopeaks was measured by XPS and the metallic ratios X_i were calculated for the stainless steel plates after acidic treatment (SSH) and after sol-gel deposition (SSHT) (Table 3). Most elements constituting stainless steel (Fe, Mo, Mn) are still observed on SSHT. Iron oxide is the major compound in the ~10 nm depth analysed. As expected, the surface composition has been strongly modified by the coating of TiO_2 as well as by the calcination step. Indeed, the amount of Fe^{3+} on SSHT is greater (×1.5), while that of Mo^{6+} is divided by 10, and some Mn^{2+} also occurs. The Cr 2p photopeak has disappeared because CrO_3, which is formed by oxidation of Cr_2O_3, is a very volatile compound escaping during calcination [31]. The Ti 2p photopeak at 458.3 eV corresponds to that of titanium oxide, and the corresponding X_{Ti} is equal to 15 %. Therefore, the surface of SSHT is better described as constituted by Fe^{3+} and Ti^{4+} oxides, and not only by TiO_2 as expected.

This finding was confirmed by XRD on SSH and SSHT plates. On SSHT diffractogram (Figure 4) the lines of the austenitic phase of stainless steel [32] are superimposed to those of α–Fe_2O_3 [33] and of pseudobrookite Fe_2TiO_5 in small amounts. Only Fe_2O_3 spectrum was observed when SSHT plates were examined by Raman spectroscopy.

In conclusion, the immersion of SSH plates in the titania sol-gel followed by calcination at 900°C did not result only in the formation of an anchoring layer of TiO_2, as expected. A mixture of iron oxide and Fe_2TiO_5, the latter being certainly formed by the high temperature reaction between Fe_2O_3 and TiO_2, was also present.

3.2. TiO_2/stainless steel plates (T/SSHT)

Once dip-coated in the suspension of TiO_2, T/SSHT plates were calcined up to 900°C. This temperature was chosen after dilatometric experiments performed on the Aldrich powder of TiO_2-anatase. The powder was pressed (1 t/cm²) in order to obtain a cylinder (diameter: 5mm, L_0 = 4.95 mm), which was placed in a furnace and gradually compressed while the temperature increased at 5°C/min rate.

Figure 5 shows that the cylinder expanded little between 200 and 850°C. When calcination of plates was performed at temperatures between 450 and 800°C, the resulting films did not satisfy the mechanical and chemical tests. The sintering begins ca. 900°C, temperature at which TiO_2 cylinder loses 0.6 % length. We assume that at this temperature the interactions plates/powders are strong enough, so that the strength of adhesion increases.

To show that little modification of the physicochemical properties (specific surface area, crystallographic structure) of TiO_2-anatase occurred during calcination, both TiO_2 powder and T/SSHT plates were analysed by several techniques and their properties were compared.

A thermobalance was used to determine the texture of the film on T/SSHT. Several plates were prepared, and cut in 6 cm² pieces. Results showed that the development factor (m²/ m² geometric surface) was equal to 300 m²/m². The specific surface area of the TiO_2 film was determined on the resulting powder (about 30 mg) after that the film had been scratched on both sides of the plates. The specific surface area was found similar to that obtained for the genuine powder, ca. 10 m²/g. Furthermore, ten T/SSHT plates were prepared and their titania films were scratched successively and collected. The average weight of anatase on each plate was found to be

29 ± 1 mg, which confirms that the deposition method is reproducible.

Aldrich powder initially contains potassium and phosphorus impurities, as shown by XPS. The BE of K 2p (293.2 eV) and P 2p (133.4 eV) photopeaks (Table 4) corresponds to K^+ in potassium oxide and P^{5+} in P_2O_5, respectively. These oxides are still present in T/SSHT plate but in lesser amounts. The K/Ti and P/Ti ratios have slightly decreased, probably because the corresponding oxides have been partly dissolved in water during the suspension step [34]. The other elements like Fe, Cr…, constituting stainless steel plates were not observed, which means that the thickness of the TiO_2 film is higher than 10 nm. The SEM micrograph of T/SSHT confirmed that TiO_2 film was 15 µm thick (Figure 6).

Finally, Raman spectroscopy carried out on T/SSHT after calcination showed that anatase was still present. XRD pattern of the scratched powder exhibited mostly the lines of anatase, although a small amount of rutile was detected (approximate anatase/rutile ratio = 97/3). Therefore, the high temperature (900°C) at which the plates were calcined so as to get stable films did not strongly modify the crystallographic structure and the porous texture of TiO_2 (Aldrich).

3.3. VO_x/TiO_2/stainless steel plates (VT/SSHT).

Due to the shape of the plates, the traditionnal impregnation techniques used for deositing VO_x on powder catalytic supports (such as incipient wetness technique) cannot be considered. The reaction between the surface TiO_2 hydroxyl groups with vanadia precursor molecules is therefore the best route to obtain well defined surface concentrations of vanadium. Here, two cases are possible: i) a very reactive precursor will react with all surface hydroxyls leading to monolayer coverage, or ii) a less reactive precursor will lead to an equilibrated reaction allowing the control of the surface

concentration of VO_x specie, up to the monolayer. The latter option was choosed in this work. The difficulty met for determining the number of hydroxyl specie at the surface of the catalyst was overcome by an extensive use of XPS characterization. Indeed, XPS was used to determine at which concentration ($0.5 < C < 4$ wt%) of the VO_x precursor in ethanol the "theoretical monolayer" is reached on VT/SSHT plates. The binding energy and Full Width at Half Maximum (FWHM) of V $2p_{3/2}$ and Ti $2p_{3/2}$ photopeaks (Table 5) were in good agreement with the literature data for the V_2O_5/TiO_2 system [35], and were practically unchanged compared to those of pure V_2O_5 and TiO_2 oxides. The small differences observed for FWHMs came from the fact that TiO_2 (Aldrich) contains potassium. Potassium oxide is known to modify the redox properties of vanadium in VO_x species, because it increases the stability of V^{5+} [36]. Other values in Table 5 stand for VO_x/TiO_2 powders (prepared with TiO_2 Alfa-Aesar) and $VO_x/TiO_2/Al_2O_3/Al$ plates [8] for comparison.

In all cases, the variation of V/Ti ratio depends on the range of VO_x precursor concentration C. V/Ti increases steadily with $0.5 < C < 2.0$, and reaches a plateau at V/Ti = 0.2 as shown on Figure 7. A further increase of C ($C \geq 3.5$) leads to a sharp increase of V/Ti corresponding to the precipitation of V_2O_5, which is not represented in Figure 7 for the sake of clarity. The same plateau at V/Ti = 0.2 ratio was found when VO_x was grafted on TiO_2 films coating anodised aluminum plates [8](also reported in Table 5 and Figure 7).

Such a V/Ti (0.2) value is also reported in the literature for powders when a monolayer of VO_x is reached. Bond et al. [37, 38] have demonstrated that, as the V loading increases, the formation of the polyvanadate monolayer is followed by the building of a disordered VO_x phase in the one-to-four monolayers equivalent range, and

then by paracrystalline V_2O_5 exposing mainly planes perpendicular to the basal [010] plane. These blocks, which grow into microcrystalline "towers", cover only a limited part of the surface resulting in a change in the slope of the V/Ti curve vs loading at the monolayer. Bond et al. [37-39] and Mendialdua et al. [40] observed such an inflexion point at V/Ti = 0.2 and 0.3, respectively. For the sake of comparison, we have prepared several samples of VO_x/TiO_2 varying by the V_2O_5/TiO_2 weight ratio. TiO_2 powder (Alfa Aesar, 50 m^2/g) was impregnated by various amounts of NH_4VO_3 in oxalic acid solution and calcined under air flow at 450°C in the same conditions as plates. In this case, the theoretical monolayer should be reached for V_2O_5/TiO_2 = 3.5 wt%. By XPS (Table 5 and Figure 7), we observe indeed that V/Ti increases linearly up to 0.2 for V_2O_5/TiO_2 below 3.5 wt% , after which value the slope is far smaller.

We may therefore deduce that the plateau observed for plate samples at V/Ti = 0.2 indeed corresponds to the monolayer and that the ratio characterizing VO_x monolayers when supported by TiO_2 is independent from the shaping of the anatase support (powder or plate). The grafting method thus allows a better control of the amount and dispersion of the VO_x specie on the TiO_2 surface up to the monolayer. This is a very important point, as the control of the amount of vanadium oxide deposited on TiO_2 is crucial for the catalytic properties of the material.

4. Conclusion

In a previous paper, we had exposed the difficulties we faced when trying to deposit a porous film of TiO_2 on anodised aluminum plate because titania did not enter the pores. Another method has been adopted to coat stainless steel, which is the preferred material of industrial catalytic reactors, by taking advantage of its excellent thermal resistance as compared to aluminum. An anchoring layer of TiO_2 was grafted

by dip-coating of passivated plates in Ti alkoxide sol-gel and further consolidated by calcination at 900°C. The SSHT plates were dipped in an aqueous suspension of Aldrich TiO_2 powder which was selected because of its narrow granulometric range. After optimisation of the conditions of coating and assessing the chemical and mechanical stability, a stable TiO_2 film of 15 μm thickness was reproducibly obtained. The physicochemical properties of the initial commercial powder were retained in the final film, among which the specific surface area (10 m^2/g). Finally, VO_x specie were grafted onto T/SSHT using vanadyl-alkoxy sol-gel medium, followed by calcination at 450°C. We have therefore demonstrated that the dip-coating technique using metallic alcoholates and titania suspension is a valuable method for the coating of VO_x/TiO_2 on flat stainless steel plates. Although more complicated geometric shapes of the metallic support may affect the properties of the porous layer of TiO_2 (thickness, adhesion) and are worth to be further investigated, we do not expect that it may affect the grafting of the active phase. We have also emphasized that catalytic deposits on metallic plates are not straightforwardly realized nor characterized as compared to the well characterized powders of VO_x/TiO_2 catalyst. Whereas on powder catalysts the surface V/Ti composition is directly determined by the stoichiometry of the impregnation solution, this is not the case when using metallic carriers. This difficulty was overcome here by the extensive use of XPS at every stage of the process. Finally, most physico-chemical properties of the VO_x/TiO_2 system were retained. The composition corresponding to the formation of VO_x monolayers on anatase is in good agreement with that found in the literature for powders, as well as with that obtained for $VO_x/TiO_2/Al_2O_3/Al$ plates, demonstrating thereby that the shaping of anatase (powder or plate) has not modified the properties of the VO_x/TiO_2-anatase system. The catalytic properties of these systems in the oxidative dehydrogenation of propane to propene [30] will be the matter of a

forthcoming paper.

Acknowledgements

L. Gengembre and M. Frère are thanked for XPS experiments and discussion.

References

[] K.F. Jensen, Chem. Eng. Sci. 56 (2001) 293.

[2] J.J. Lerou, M.P. Harold, J. Ashmead, T.C. O'Brien, M. Johnson, J. Perrotto, C.T. Blaisdell, T.A. Rensi, J. Nyquist, Microsystem technology for chemical and biological microreactors. Dechema monographs, 132 (1996) 51.

[3] M. Merzouki, E. Bordes, B. Taouk, L. Monceaux, P. Courtine, Stud. Surf. Sci. Catal. 72 (1992) 165.

[4] M. Merzouki, B. Taouk, L. Tessier, E. Bordes, P. Courtine, New Frontiers in Catalysis, L. Guczi et al. (Eds.), 1993, p.753.

[5] L. Tessier, E. Bordes, M. Gubelmann-Bonneau, Catal. Today 24 (1995) 340.

[6] F. Arena, F. Frusteri, A. Parmaliana, Cat. Lett. 60 (1999) 59.

[7] L. Kiwi-Minsker, A. Renken, Catal. Today 110 (2005) 2.

[8] T. Giornelli, A. Löfberg, E. Bordes-Richard, Thin Solid Films 479 (2005) 64.

[9] F. Vacandio, M. Eyraud, Y. Massiani, Bulletin de l'Union des Physiciens, 97 (2003)

1.

[10] A. Mills, J. Wang, J. Photochem. Photobiol. A: Chem. 118 (1998) 53.

[1] S. Kambe, K. Murakoshi, T. Kitamura, Y. Wada, S. Yanagida, H. Kominami, Y. Kera, Sol. Energy Mater. Sol. Cells 61 (2000) 427.

[2] R. Fretwell, P. Douglas, J. Photochem. Photobiol. A: Chem. 143 (2001) 229.

[3] I. Zumeta, R. Espinosa, J. A. Ayllón, X. Domènech, R. Rodríguez-Clemente, E. Vigil, Sol. Energy Mater. Sol. Cells 76 (2003) 15.

[4] R. Fretwell, P. Douglas, J. Photochem. Photobiol. A: Chem. 143 (2001) 229.

[5] S. Horikoshi, N. Watanabe, H. Onishi, H. hidaka, N. Serpone, Appl. Catal. A: Gen. 37 (2002) 117.

[6] J. Yu, J.C. Yu, W. Ho, Z. Jiang, New. J. Chem. 26 (2002) 607.

[7] P. Chrysicopoulou, D. Davazoglou, C. Trapalis, G. Kordas, Thin Solid Films 323 (1998) 188.

[8] A. Fernandez, G. Lassaletta, V. M. Jimenez, A. Justo, A. R Gonzalez-Elipe, J. M. Herrmann, H. Tahiri, Y. Ait-Ichou, Appl. Catal. B: Environ. 7 (1995) 49.

[9] J. A. Byrne, B. R. Eggins, N. M. D. Brown, B. Mc Kinney, M. Rouse, Appl. Catal. B: Environ 17 (1997) 25.

[20] G.C. Bond, Appl. Catal. A: Gen. 157 (1997) 91

[21] K. Haas-Santo, M. Fichtner, K. Schubert, Appl. Catal. A: Gen. 220 (2001) 79.

[22] I. Olefjord, B. O. Elfstrom, Corrosion 38 (1982) 46.

[23] K. Varga, P. Baradlai, W. O. Barnard, G. Myburg, P. Halmos, J. H. Potgieter, Electrochim. Acta. 42 (1997) 25.

[24] S. Kannan, A. Balamurugan, S. Rajeswari, Mat. Lett. 57 (2003) 2382.

[25] J. K. Heuer, J. K. Stubbins, Corros. Sci., 41 (1999) 1231.

[26] P. Stefanov, D. Stoychev, M. Stoycheva, T. Marinova, Mat. Chem. Phys. 65 (2000) 212.

[27] A. Mills, J. Wang, J. Photochem. Photobiol. A: Chem. 118 (1998) 53.

[28] R. Fretwell, P. Douglas, J. Photochem. Photobiol. A: Chem. 143 (2001) 229.

[29] I. Zumeta, R. Espinosa, J. A. Ayllòn, X. Domènech, R. Rodrìguez-Clemente, E. Vigil, Sol. Energy Mater. Sol. Cells 76 (2003) 15.

[30] T. Giornelli, Ph.D. Thesis, Université de Technologie de Compiègne, France, 2005.

[31] F. J. Perez, F. Pedraza, M. P. Hierro, J. Balmain, G. Bonnet, Surf. Coat. Technol. 153 (2002) 49.

[32] R. K. Zalavutdinov, Y. Dai, A. E. Gorodetsky, G. S. Bauer, V. K. Alimov, A. P. Zakharov, J. Nucl. Mat. 296 (2001) 219.

[33] F. Riffard, H. Buscail, E. Chaudron, R. Cueff, C. Issartel, S. Perrier, Mat. Charac. 49 (2002) 55.

[34] D. Courcot, Ph.D. Thesis, Université des Sciences et Technologies de Lille, France, 1994.

[35] J.C. Védrine, Catal. Today 20 (1994) 109.

[36] A. J. Van Hengstum, J. Pranger, J. G. Van Ommen, P. J. Gellings, Appl. Catal. 11 (1984) 317.

[37] G.C. Bond, P. Köning, J. Catal. 77 (1982) 309.

[38] G.C. Bond, J. Perez Zurita, S. Flamerz, P.J. Gellings, H. Bosch, J.G. Van Ommen, Appl. Catal. 22 (1986) 361.

[39] G.C. Bond, J. Perez Zurita, S. Flamerz, Appl. Catal. 27 (1986) 353.

[40] J. Mendialdua, Y. Barbaux, L. Gengembre, J. P. Bonnelle, B. Grzybowska, M. Gasior, Bull. Pol. Acad. Sci. Chem. 35 (1987) 213.

Figure captions:

Figure 1: Bi-layer model of the passive film on stainless steel

Figure 2: SEM micrographs (× 5000) : stainless steel surfaces before (a) and after (b) acidic treatment

Figure 3: SEM micrographs (× 2500) : stainless steel surfaces of SSH after acidic treatment (a) and SSHT after grafting of TiO_x (b)

Figure 4: Diffractograms of SSH (a) and SSHT (b) plates: austenite (◊), Fe_2O_3 (*) , Fe_2TiO_5 (•)

Figure 5: Dilatometric analysis of TiO_2-Aldrich powder

Figure 6: SEM micrograph of T/SSHT showing the film of TiO_2

Figure 7: XPS experiments on VO_x/TiO_2 coated on plates or as powder. V/Ti intensity ratio vs. concentration of the grafting solution for plates (bottom X axis: $VO(OPr)_3$ wt% in ethanol; Δ: VT/SST; :$VO_x/TiO_2/Al_2O_3$/Al plates [8]) and vs VO_x loading for powders (top X axis: V_2O_5/TiO_2 wt%) (◊).

Table captions:

Table 1 : Chemical composition of the stainless steel 316L.

Table 2 : XPS analysis of stainless steel plates before and after acidic treatment. Binding energy (BE) of Fe 2p, Cr 2p, Mo 3d and metallic ratios X_i.

Table 3: Binding energy (BE) of Fe, Ti, Mo, Cr, Mn and metallic ratio X_i for the stainless steel plates after the acidic treatment (SSH) and after the sol-gel deposition (SSHT).

Table 4: XPS analysis of TiO_2 powder and of T/SSHT plates. Binding energy (BE) of Ti 2p, P 2p, K 2p photopeaks and atomic ratio M/Ti.

Table 5: XPS analysis of VT/SSHT plates and comparison with VO_x/TiO_2/Al plates and VO_x/TiO_2 powders. Binding energy (BE ± 0.2 eV) and Full Width at Half Maximum (FWHM) (eV) of V $2p_{3/2}$ and Ti $2p_{3/2}$. V/Ti is the ratio of intensity of V 2p3/2 to Ti $2p_{3/2}$ photopeaks. (C= $VO(OPr)_3$ wt% in ethanol; F= V_2O_5/TiO_2 wt%)

Table 1

Elements	C	Mn	P	S	Si	Ni	Cr	Mo
Maximum content (%)	0.03	2.00	0.04	0.03	1.00	13.00	18.00	2.50

Table 2

	Before H_2SO_4		After H_2SO_4	
Photopeaks	BE(eV)	X_i	BE(eV)	X_i
Fe 2p	711.0	0.80	711.0	0.47
Mo 3d	233.0	0.03	232.8	0.06
Cr 2p	577.1	0.15	577.4	0.47

Table 3

Photopeaks	SSH		SSHT	
	BE (eV)	X_i	BE (eV)	X_i
Fe 2p	711.0	0.50	711.1	0.75
Ti 2p	-	-	458.3	0.15
Mo 3d	232.8	0.06	232.4	0.005
Cr 2p	577.4	0.50	-	-
Mn 2p	-	-	641.5	0.07

Table 4

Photopeaks	TiO_2 (Aldrich)		T/SSHT	
	BE (eV) ± 0,1	Atomic ratio M/Ti	BE (eV) ± 0,1	Atomic ratio M/Ti
Ti 2p	458.7	1	458.8	1
P 2p	133.4	0.1	133.4	0.07
K 2p	293.2	0.1	293.2	0.08

Table 5

Catalysts	V $2p_{3/2}$		Ti $2p_{3/2}$		O 1s		V/Ti
	BE	FWHM	BE	FWHM	BE	FWHM	
VT/SSHT plates							
C = 0.5-3.0	517.4	1.5	458.9	1.2	530.0	1.8	0.05-0.195
C = 3.5-4.0	517.5	1.5	458.9	1.2	530.0	1.8	0.28-0.41
VO_x/TiO_2/Al plates [8]							
C = 0.5-2.2	517.0	2.0	458.8	1.6	530.0	1.8	0.1 -0.2
C = 2.4-8	517.2	1.8	458.9	1.6	530.0	1.8	0.3 -8.0
VO_x/TiO_2 powder							
F = 0.5-3.5	517.3	1.9	458.6	1.2	530.0	1.8	0.1 -0.2
F = 6.25-20	517.4	1.4	458.6	1.2	530.0	1.8	0.31-0.62
TiO_2 [35]	-		458.7	1.3	529.9	1.6	-
V_2O_5 [35]	517.4	1.5	-	-	530.2	1.5	-
[40]	517.0	1.4			530.0	1.6	

Figure1

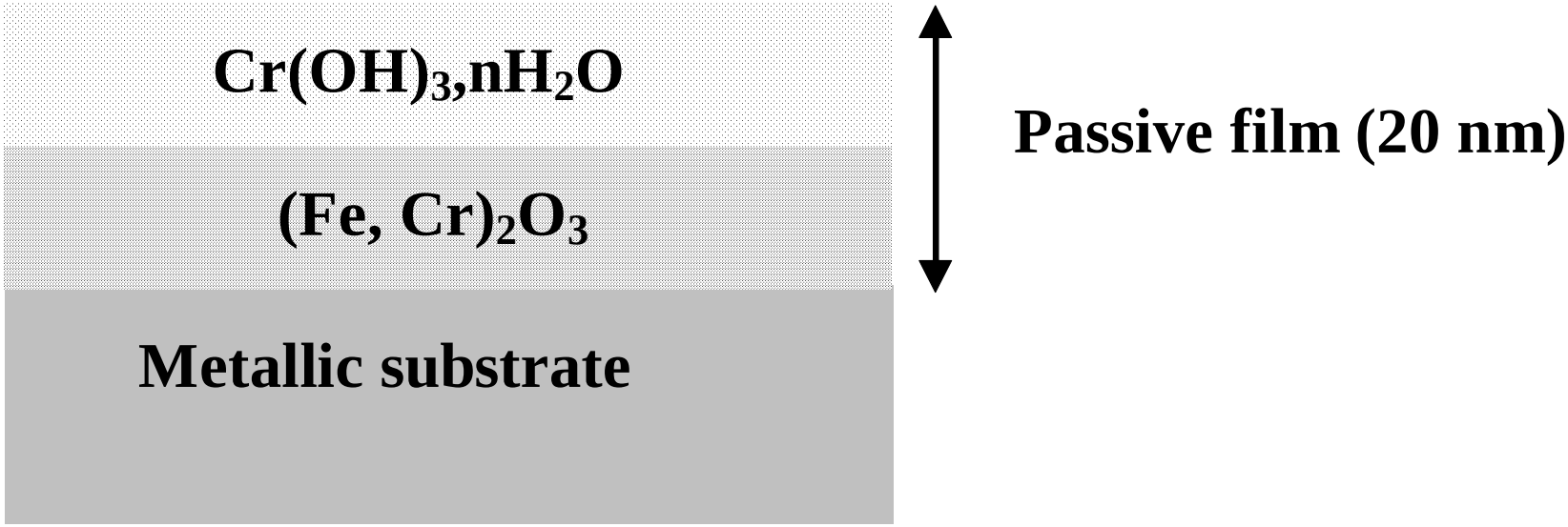

Figure2

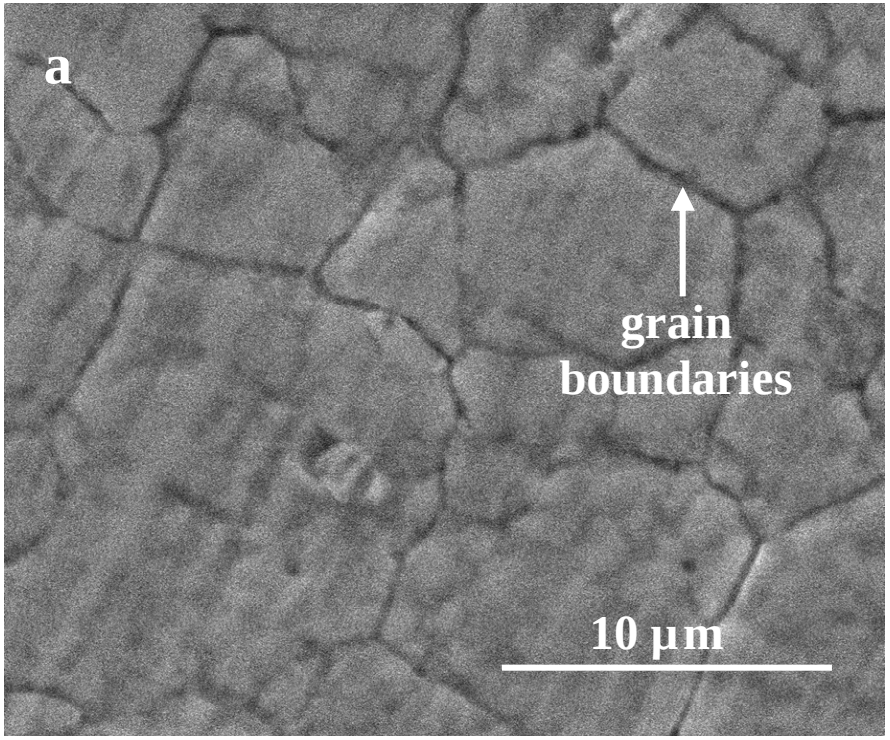

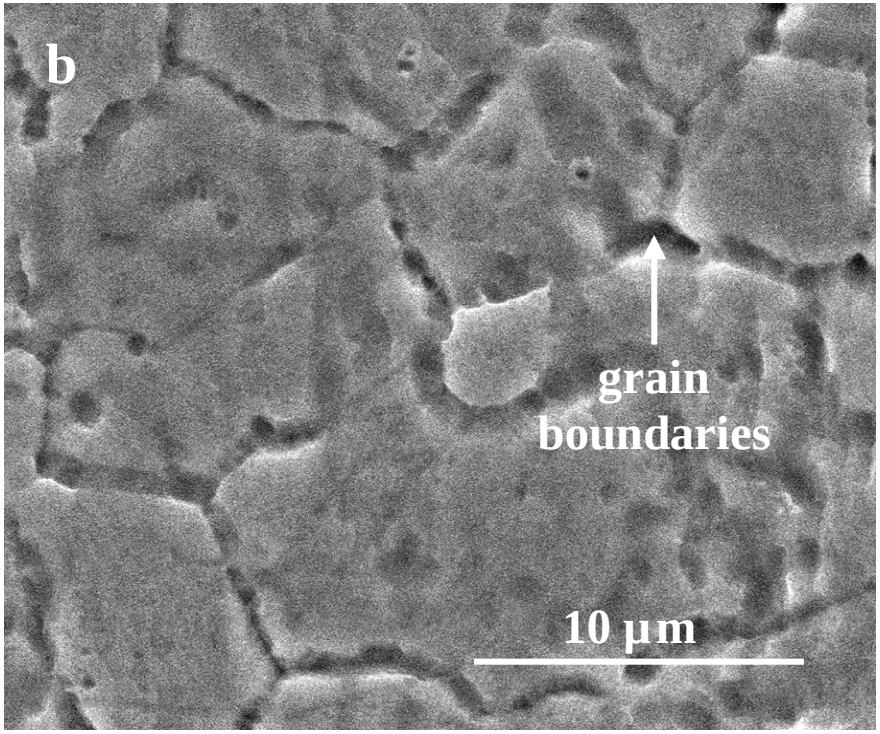

Figure3

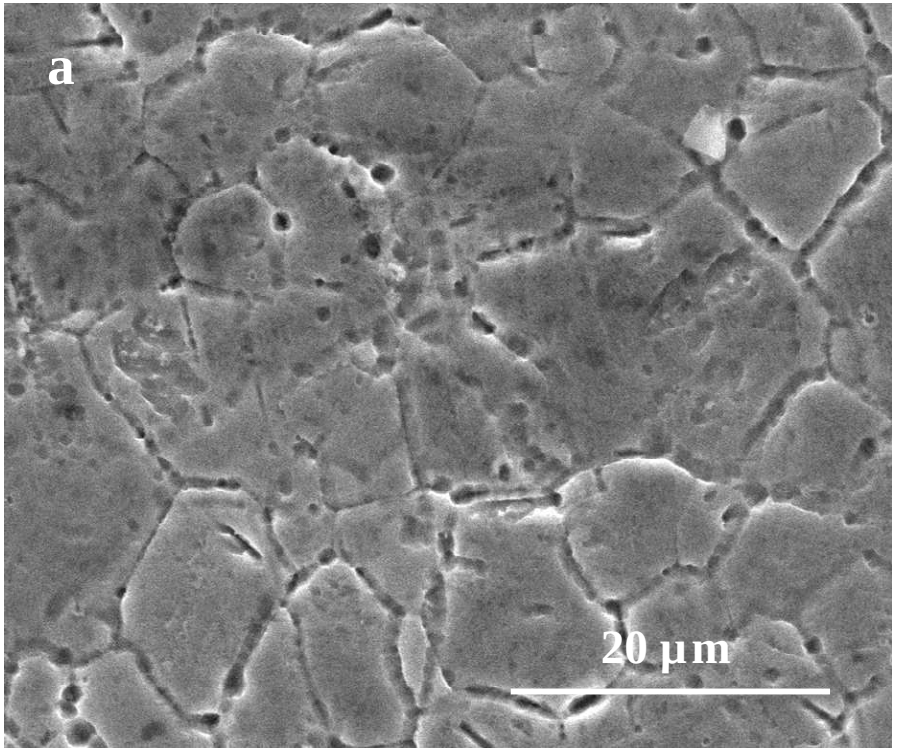

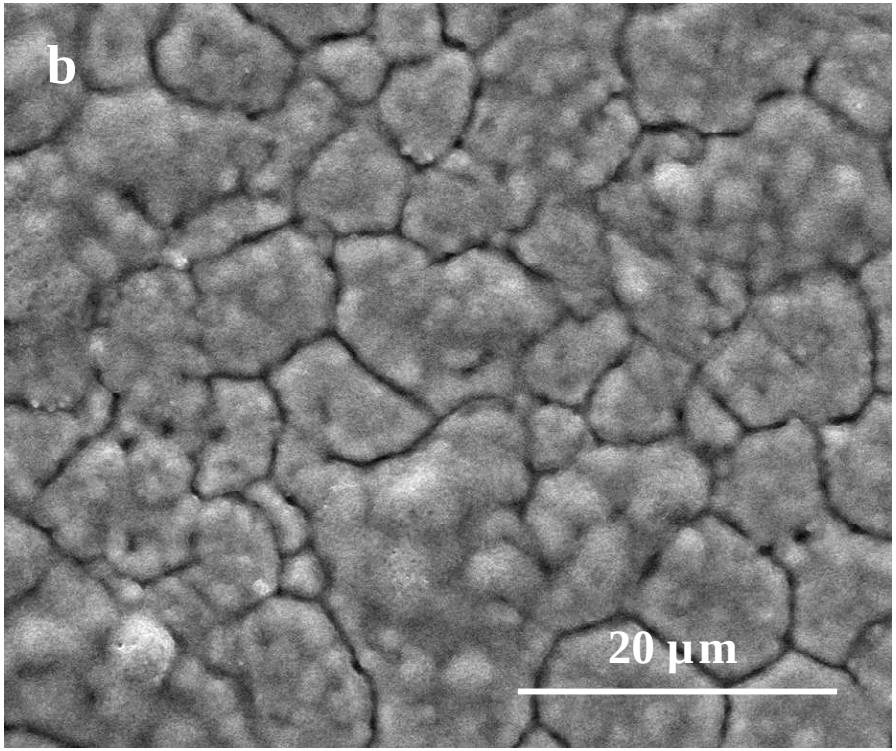

Figure4

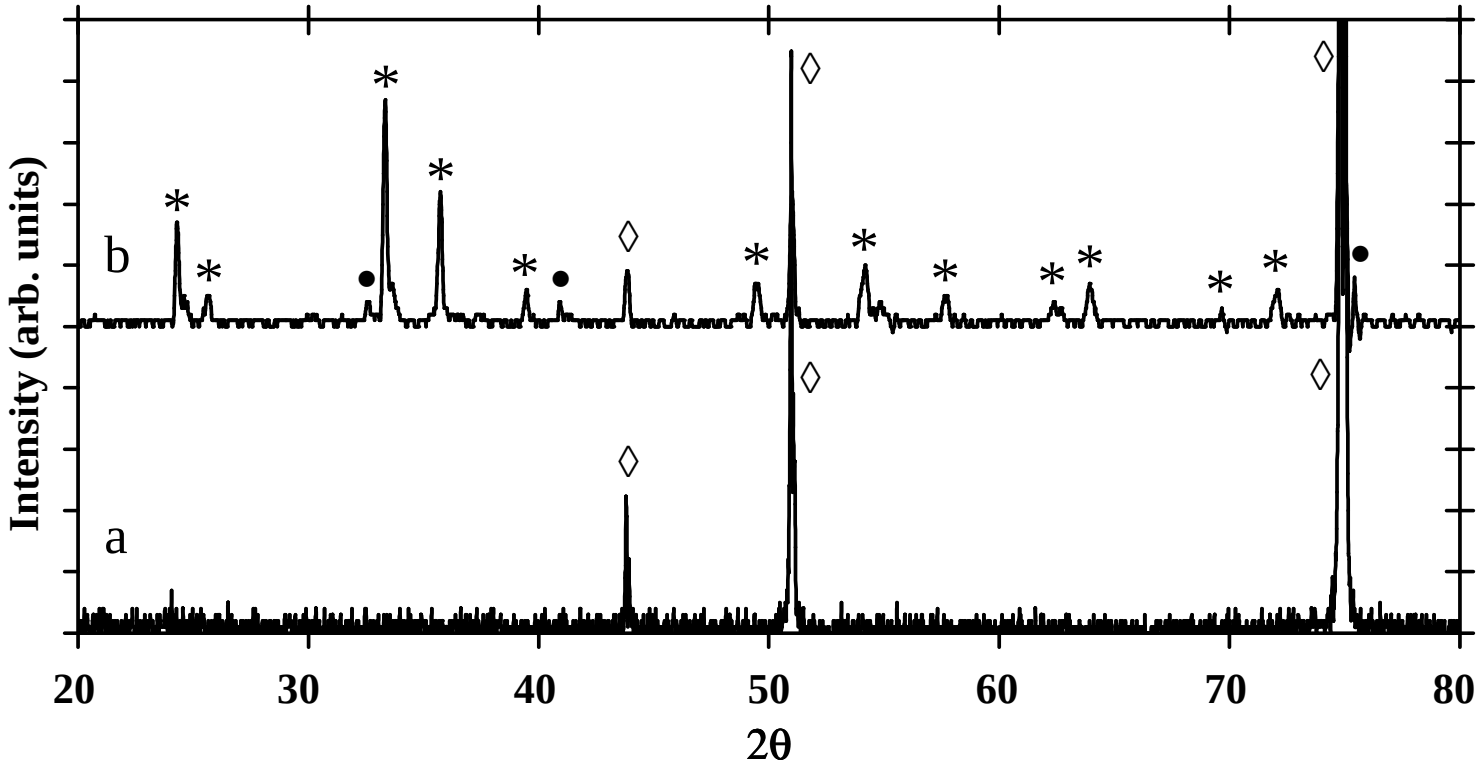

Figure5

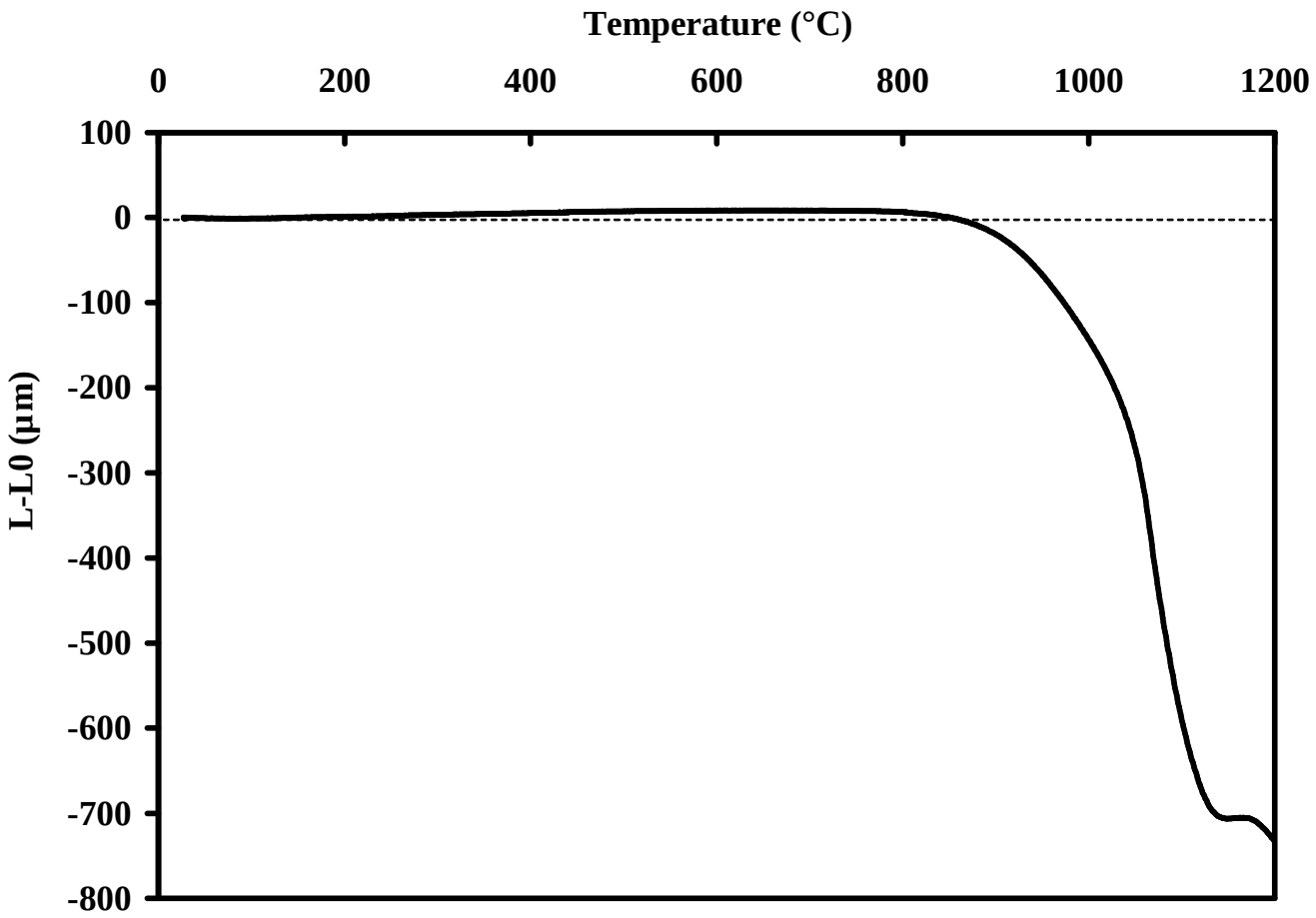
Temperature (°C)
0
200
400
600
800
1000
1200
100
0
-100
-200
-300
-400
-500
-600
-700
-800
L-L0 (μm)

Figure6

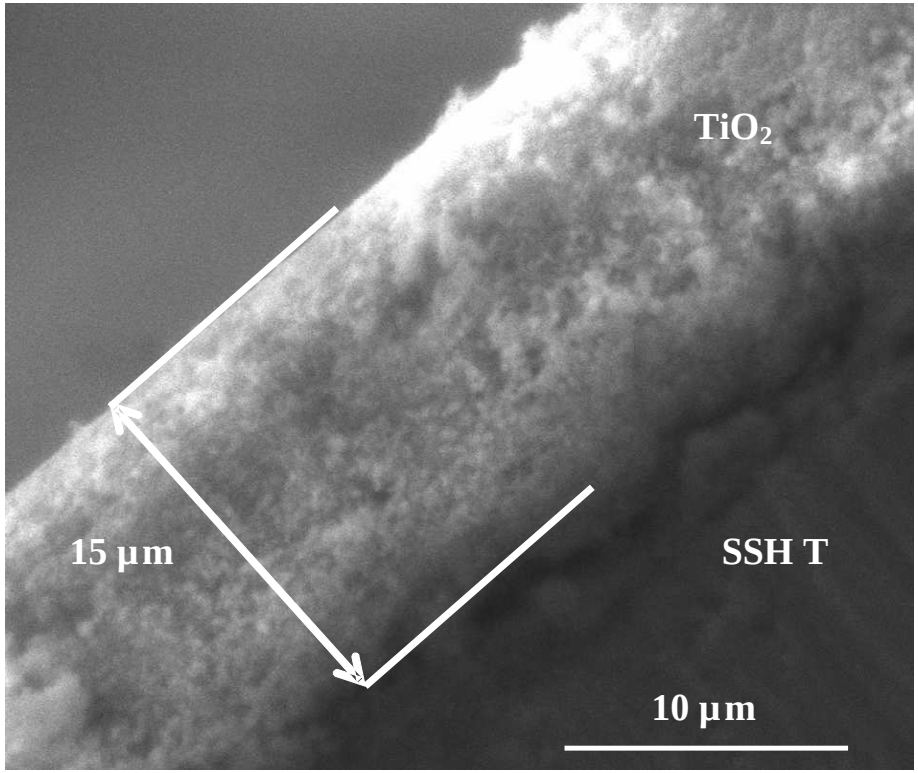

Figure7

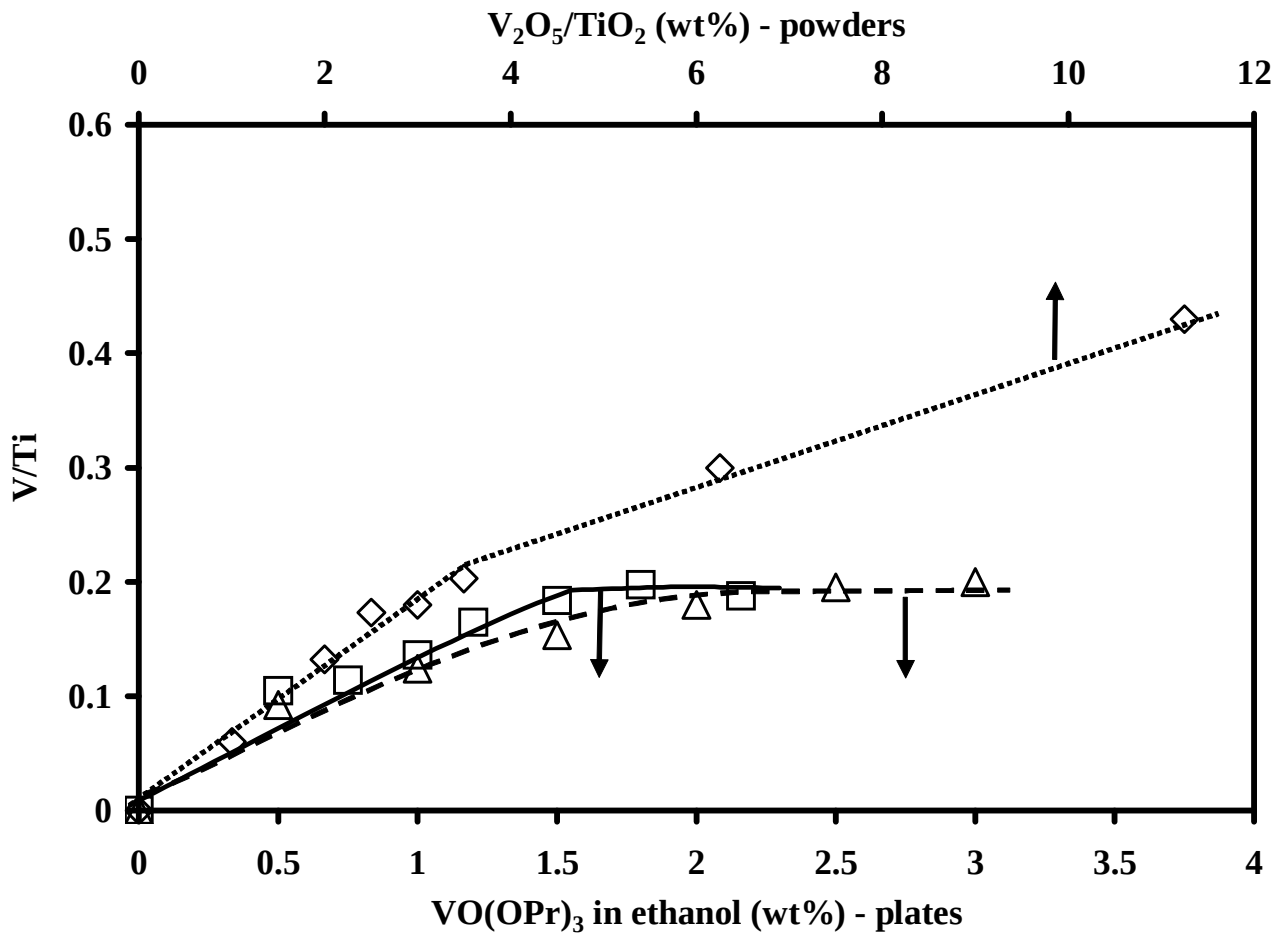
V2O5/TiO2 (wt%) - powders
0
2
4
6
8
10
12
0.6
0.5
0.4
0.3
0.2
0.1
0
V/Ti
0
0.5
1
1.5
2
2.5
3
3.5
4
VO(OPr)3 in ethanol (wt%) - plates